# Mexneurin is a novel precursor of peptides in the central nervous system of rodents

**Maura Epifanía Matus-Ortega**[a], **Philippe Leff Gelman**[b], **Juan Carlos Calva-Nieves**[a], **Anabel Flores-Zamora**[a], **Alberto Salazar-Juárez**[a], **Carlos-Alejandro Torner-Aguilar**[c], **Gerardo Gamba**[d], **Paola De Los Heros**[e], **Bonnie Peng**[f], **John E. Pintar**[f], **Heinrich S. Gompf**[g], **Charles N. Allen**[g], and **Benito Antón-Palma**[a,†]

[a]Instituto Nacional de Psiquiatría Ramón de la Fuente Muñiz. Calzada México-Xochimilco #101. 14370. Ciudad de México. México

[b]Instituto Nacional de Perinatología, Montes Urales # 800, 11000. Ciudad de México. México

[c]Departamento de Atención a la Salud, C.B.S., UAM, Calzada del Hueso 1100, Col. Villa Quietud, Delegación Coyoacán, 04960, Ciudad de México. México

[d]Molecular Physiology Unit, Instituto Nacional de Ciencias Médicas y Nutrición Salvador Zubirán and Instituto de Investigaciones Biomédicas, Universidad Nacional Autónoma de México, Tlalpan, Ciudad de México, 14000, México

[e]Dirección de Investigación, Facultad de Medicina, Universidad Nacional Autónoma de México. Coyoacán, 04320, Ciudad de México, México

[f]Department of Neuroscience and Cell Biology, Rutgers Biomedical and Health Sciences, Newark, NJ, USA

[g]Oregon Institute of Occupational Health Sciences, Oregon Health & Science University, 3181 SW Sam Jackson Park Road, Portland, OR 97239, USA

## Abstract

Endomorphins have been proposed as the endogenous ligand agonists of the μ-opioid receptor; however, no propeptide precursor protein for endomorphins has been identified. Here, to identify the presumed precursor of endomorphins, we designed an immunoscreening assay using specific affinity-purified rabbit antisera raised against synthetic endomorphins in a whole mouse brain cDNA library. Following this approach, we identifiy a DNA sequence encoding a protein precursor, which we name proMexneurin, that contains three different peptide sequences: Mexneurin-1 (an endomorphin-like peptide), Mexneurin-2, and Mexneurin-3, a peptide which

Corresponding author: Maura Epifanía Matus-Ortega. Instituto Nacional de Psiquiatría Ramón de la Fuente Muñiz. Calzada México-Xochimilco #101. 14370. Ciudad de México. México. Tel: 252 4160 5115. Fax: mematuso@gmail.com.
†Deceased 3 March 2016.

appears to be unrelated to endomorphins. RT-PCR analysis and in situ hybridization reveal a widespread distribution of proMexneurin mRNA throughout the mouse brain. Both Mexneurin-1 and Mexneurin-3 peptides display biological activities in the mouse CNS.

## Keywords

Opioid peptides; Protein precursor; Endomorphin

## 1. Introduction

Opioid peptides comprise a family of active neuropeptides and neurohormones that are processed from large precursor proteins known as pro-opiomelanocortin, pre-proenkephalin and pre-prodynorphin [1]. All opioid peptides share a common N-terminal sequence (Tyr-Gly-Gly-Phe-Leu/Met) which interacts with the mu, delta and kappa receptors [2]. Several endogenous opioids have been reported: the orphanin FQ peptide which binds to the ORL-1 receptor [3, 4], and the endomorphins (EMs), consisting of EM1 and EM2 amide tetrapeptides, and displaying a high binding affinity and selectivity to the mu-opioid receptor (MOR) [5, 6, 7]. EMs peptides exert a broad spectrum of modulatory bioactivities at both neuroendocrine and cardiovascular systems, including mood, feeding, reproduction, sexual behavior, and pain [8, 9, and 10]. Thus, mature EMs are crucial molecules implicated in the regulation of several physiological activities and behaviors in mammalian species; however, its propeptide precursor(s) remain yet to be identified. In 2007, Terskiy and colleagues performed a bioinformatic study, searching in the current human proteome for putative endomorphin precursor proteins. Such proteome screening yielded no evidence for endomorphin precursor protein based on accepted biochemical criteria [11]. Thus, there is no convincing evidence that an endogenous precursor protein for EMs is encoded in the mammalian genome. Given the lack of information about the EM peptide precursor and the availability of specific affinity-purified rabbit antisera raised against either EM1 or EM2 peptides [12], we decided to pursue an immunological strategy.

## 2. Material and methods

### 2.1 Drugs and Peptides

Synthetic peptides of EM1 (5 mg), EM2 (5 mg), naloxone and DAMGO were purchased from Tocris, USA. Mexneurin-1 (Mx-1) was custom synthesized from Biosynthesis Inc. USA.

### 2.2 Animals

All studies were conducted in accordance with animal care ethics approval and guidelines, as outlined by the National Institutes of Health (NIH, Guide for Care and Use of Animals) and approved in advance by NOM-062-ZOO-1999 (Mexico City) and the Oregon Health & Sciences University Institutional Animal Care and Use Committee. Animals were housed in plastic cages at $22 \pm 2°$ C with a 12:12 h light-dark cycle (08:00 on; 20:00 off) in a temperature-controlled room with food and water *ad lib*. Male BALB/c mice were used for

RT-PCR assays (25–35g) and male Wistar rats (180–220 g) for [$^{35}$S]GTP$\gamma$S binding assays and Sprague Dawley rats for electrophysiological studies.

### 2.3 Immunoscreening

Polyclonal antibodies from rabbits, previously reported [12], were used against the synthetic EMs. Both antisera, C-14 raised against EM1 (Tyr-Pro-Trp-Phe-NH$_2$) and C-16 raised against EM2 (Tyr-Pro-Phe-Phe-NH$_2$) were used for immunoscreening a whole mouse brain cDNA library (Lambda - ZAP, Stratagene) expressed in XL1-Blue MRF' *E. coli* strain. A total of $1 \times 10^9$ plaques were screened according to the manufacturer instructions. The dilution of each serum was 1:20. Bound antibodies were detected with a $^{125}$I–conjugated Goat Anti-Rabbit IgG, Fc fragment specific secondary antibody. Positive plaques were excised from the plate and submitted to two further rounds of immunoscreening until purity was achieved. Positive clones were excised to pBlueScript-SK+ plasmid forms according to the manufacturer instructions (Stratagene). Positive clones identified were PCR amplified using T3 and T7 vector-specific primers (Gibco/BRL) and was sequenced using the BigDye Terminator Cycle Sequencing kit on an AbiPrism 310 Genetic Analyzer (Applied Biosystems).

### 2.4 Nucleotide and amino acid sequence analysis

The BLASTn, BLASTp and FASTA searches (http://www.ncbi.nlm.nhi.gov and www.ebi.ac.uk) were used for analysis of cDNA and protein sequences. Protein translation was done using BioEdit v7 Sequence Alignment Editor Software. Prediction of translation initiation ATG was done by ATGpr at website http://atgpr.dbcls.jp/. The sORFfinder program was used to confirm the open reading frame (ORF) at http://evolver.psc.riken.jp/. Putative protein parameters were analyzed using the tools from ExPaSy Molecular Biology Server (http://www.expasy.org/). SignalP (http://www.cbs.dtu.dk/Services/SignalP/) was used to predict classical secreted proteins and the SecretomeP 2.0 software (http://www.cbs.dtu.dk/Services/SecretomeP2.0/) was used to predict mammalian secretory protein targeted to the non-classical secretory pathway. We used the Neuropred software (http://www.neuroproteomics.scs.uiuc.edu/neupred.html), a tool designed to predict cleavage sites at pair of basic amino acid residues along the primary sequence of neuropeptide precursors [13].

### 2.5 Tissue extraction of RNA and reverse transcriptase reaction

Total RNA was extracted from the mouse brain and peripheral tissues using TriPure Isolation Reagent (Roche Diagnostics, IN, USA) according to the manufacturer instructions. RNA samples were reversely transcribed from 2 μg of total RNA with M-MLV Reverse Transcriptase (NE Biolabs) using oligo (dT) 9 as primers at 37° C for 1.0 h, according to the manufacturer instructions. Polymerase chain reaction (PCR) amplification was executed using 5 μl of the cDNA, 1.25 U of Taq DNA polymerase (Invitrogen), 0.1 mM of each dNTP (Gibco/BRL), 2.5 mM MgCl$_2$ (Gibco/BRL) and 0.4 μM of each primer. Primer sequences, MxS: 5′-TAG ATG GAC GGG CGT CAT CTA C-3′ and MxA: 5′-ACT CCG TGA CGT GTC AGA AT-3′ were synthesized to cover the whole coding region of the mouse proMexneurin mRNA and partial 3′UTR. For detection of GAPDH sequences following primers were used: forward, 5′-ACC ACA GTC CAT GCC ATC AC-3; reverse, 5′-TCC

ACC ACC CTG TTG CTG TA-3′. The amplification profile involved 30 cycles of denaturation at 94° C for 1 min, primer annealing at 57° C for 1 min, and primer extension at 72° C for 90 sec. 10 μl aliquots of PCR products were fractionated by electrophoresis in 30% polyacrylamide gels, and stained with ethidium bromide for visualization.

### 2.6 In situ hybridization studies

Studies were carried out using adult (2 months old) male BALB/c mice. Mice were deeply anaesthetized with sodium pentobarbital (50 mg/kg i.p.). Experimental tissue for *in situ* hybridization was prepared routinely by transcardial perfusion of fixative solution. Brains were flushed with 100 mI phosphate-buffered solution (pH 7.4) containing 10 mg/l heparin and then perfusion-fixed with 250 ml of 4% phosphate-buffered paraformaldehyde (pH 7.4). Fixed tissue was dissected and immersed in a solution of 30% sucrose/phospate-buffered solution/1% thimerosal at 4° C for 48 hrs. Cryoprotected tissue was embedded in OCT (Fisher Scientific), frozen on a cold solution of powdered dry ice/acetone and stored at -70° C until use. Serial sections of tissue were cut on a cryostat (Reichter Jung 2300). For *in situ* hybridization, 20 μm sections were collected on Superfrost Fisherbrand slides (Fisher Scientific) and stored at -70° C until use.

**2.6.1 Probes—**Two different cRNA probes were generated to hybridize Mexneurins (Mxs) mRNA. PCR templates were generated using Mxs specific primers with 5′ extensions of either 13 or 17 RNA polymerase promoters, a method previously described by Logel and colleagues [14]. PCR amplifications were performed according standard protocols and verified by electrophoresis. *In vitro* transcription from the PCR-generated templates was performed using the PROMEGA T7 and T3 *in vitro* Transcription Kit (Promega). The correct size of the cRNA probes was verified by electrophoresis. The labeled cRNA probes were purified by phenol/chloroform extraction and ethanol precipitation and stored in ethanol al -70° C until used. The cRNA probe generated from Mxs cDNA template was sized into fragments averaging 300–500 nucleotides long by limited alkaline hydrolysis. *In situ* hybridization was performed as described by Zheng and Pintar 1995 [15]. Areas expressing Mxs mRNAs were determined as positive after detecting grain densities at least three times higher than the background density in cell bodies. Background levels were determined from adjacent control sections hybridized with a sense cRNA probe or antisense cRNA probe in sections pretreated with RNase A.

**2.6.2 Microscopy analysis—**Brain sections were observed under bright-field illumination using a DAS LEIKA DMR Qwin-microscope. The neuroanatomical areas displaying positive hybridization signals in cells and brain regions were identified according to the atlas of the rat brain of Paxinos and Watson [16].

### 2.7 [$^{35}$S]GTP$\gamma$S binding assays

Agonist-stimulated [$^{35}$S]GTP$\gamma$S binding was assayed as previously described with slight modifications [17]. 25 μg of protein from rat hippocampus membranes was incubated for 1 h at 30° C in a final volume of 1 ml. The incubation mixture included 0.05 nM [$^{35}$S]GTP$\gamma$S and 30 μM GDP with and without maximally effective concentrations of each agonist (Mx-1, Mx-2, and Mx-3; DAMGO and EM1 as controls) in assay buffer. To test if a mu

receptor antagonist blocks the agonist effect of Mx-1 on γ-GTP incorporation, we made a γ-GTP incorporation study with saturating concentrations of naloxone (10 μM). In all experiments, basal binding was assessed in the absence of drug, and nonspecific binding was measured in the presence of 10 μM unlabelled GTPγS. All incubations were terminated by rapid filtration under vacuum through Whatman GF/B glass fiber filters, followed by three washes whit 3 ml ice-cold 50 mM Tris-HCI, pH 7.4. Bound radioactivity was determined by liquid scintillation spectrophotometry at 95% efficiency for $^{35}$S, after overnight extraction of the filters in 5 ml Scinti Verse scintillation fluid.

**2.7.1 Data analysis and statistics—**Graphs were fitted using the SigmaPlot 10.0 Software. Data are expressed as mean ± S.E.M.

## 2.8 Electrophysiological studies

**2.8.1 Preparation of brain slices—**Sprague Dawley rats (20–24 days old) were deeply anesthetized with halothane, their brains removed and submerged in ice-cold artificial cerebrospinal fluid (ASCF) containing (in mM): NaCl 87, KCl 2.5, NaH$_2$PO$_4$ 1.25, NaHCO$_3$ 25, MgCl$_2$ 7, CaCl$_2$ 0.5, glucose 25, and sucrose 75 saturated with 95% O$_2$ / 5% CO$_2$. Coronal (250 μm) slices containing the hypothalamus were prepared on a vibratome (Leica VT 1000S). Slices were transferred first to a holding chamber in which the temperature was gradually raised to 35°C over 30 min. Then, individual slices were transferred to the recording chamber in which they were completely submerged in 32° C ACSF (same as above, except MgCl$_2$ 1.2, CaCl$_2$ 2.4 mM). Experiments were performed with cells visualized using infrared differential interference contrast microscopy (IR-DIC, Leica DMLFS microscope).

**2.8.2 Patch clamp recording—**Electrodes used for patch clamp recordings had outside tip diameters of ~1 μm and resistances of ~5–8 MΩ when filled with internal solution containing (in mM): K-gluconate 110, KCl 40, MgCl$_2$ 2, HEPES 10, EGTA 0.1, ATP 2, pH 7.2. The electrode was advanced into the brain slice and a seal with the cell membrane (resistance: 2–15 GΩ) was obtained by applying negative pressure. After further negative pressure to rupture the membrane and obtain whole cell recording mode, current clamp and/or voltage clamp experiments were performed. Peptides Mx-1 (1 μM), Mx-2 (1 μM), or Mx-3 (10nM - 1 μM) were bath applied, as was the mu opioid receptor antagonist CTOP (100nM, Tocris), and the currents or voltages were measured with an Axopatch-1D amplifier (Axon Instruments, Foster City, CA) and saved on an on-line computer (Macintosh) equipped with Pulse and PulseFit software (HEKA, Lambrecht Germany). Data were analyzed in Microsoft Excel and GraphPad Prism (La Jolla, CA).

## 3. Results

### 3.1 Immunoscreening and characterization of proMexneurin mRNA

Our immunoscreening assay led to the identification of a full-length 1.083-kb cDNA clone (NCBI accession AY142705.1.). This cDNA encodes a predicted putative mature protein of 91 amino acids, which was named *proMexneurin*. An alignment analysis using the NCBI Blast+ with the nucleotide sequence showed a 100% identity with the nucleotide sequence

of the MCG119713, isoform CRA_a of *Mus musculus* and a similarity of 14 - 56% with different uncharacterized nucleotide sequences in diverse organisms such as *Cricetulus griseus*, and *Nematostella ventensis*. As shown in Fig. 1, proMexneurin cDNA consists of an ORF of 91 bp, with an initiation codon (ATG) at positions 270–272 and a stop codon (TAG) at positions 543–545. The ORF is flanked by 270 bp at the 5′ UTR and 538 bp at the 3′ UTR, respectively, which contains a polyadenylation signal ¾ 5′-AATAAA-3′ ¾ at positions 1046 to 1051 of the nucleotide sequence, ending with a poly-A tail. The protein sequence of proMexneurin protein has the NCBI accession number AAN28928. A PSI-BLAST analysis of the amino acid sequence shows a 100% identity with the MCG119713 protein sequence of *Mus musculus* (UniProtKB ID: I6L9U2_MOUSE; accession CH466552.), and a 56% of identity with an uncharacterized hypothetical protein of *Cricetulus griseus* (UniProtKB ID: G3HYP4_CRIGR and accession JH000938.1). From the deduced amino acid sequence, the N-terminal 1 to 39 residues of the consensus sequence defines a cleavage site of a signal peptide in a structural secretory protein, following the (-3, -1) von Heijne rule [18]. The predicted polypeptide appears to contain three potential mature peptides. Based on the rules of neuropeptide processing [19]; the first peptide was predicted to be a 8 amino acid peptide sequence, from residues 40–47 (Thr-8-Phe) and named *Mexneurin-1* (Mx-1), the second peptide consists of nine amino acids, corresponding to residues 50–58 (Thr-9-Ser) and named *Mexneurin-2* (Mx-2); the third predicted peptide consist of a C-terminal- 31 amino acid peptide sequence from residues 61–91 (Pro-31-Cys), and named *Mexneurin-3* (Mx-3).

### 3.2 RT-PCR amplification of the proMexneurin mRNA

PCR amplification of the proMexneurin cDNA successfully amplified a single product of 391 pb from the total RNA extracted from both neural and extra-neural tissues. As is shown in Fig. 2A, the proMexneurin gene transcript was widely expressed in mouse neuronal tissue such as the retina, olfactory bulb, cortex, hippocampus, thalamus, mesencephalon, brainstem, cerebellum, spinal cord; and from extra-neuronal tissues, such as the spleen. proMexneurin mRNA expression was not detected in non-neuronal tissues tested, such as the gut, liver, kidney and lung (data not shown).

### 3.3 Neuroanatomical distribution of proMexneurin mRNA

*In situ* hybridization revealed a widespread distribution of proMexneurin mRNA throughout the mouse brain (Fig. 2B, Fig. 2C and Supplementary data). By far, the most densely labeled areas were observed in trigeminal nerve (5n), followed by limbic structures, such as the CA3 and CA2 areas of the hippocampus and BMP; thalamic nuclei (VMP, MHb, Po, DLG), olfactory bulb (Mi) and caudate-putamen (CPu), respectively. Moderate to low mRNA densities were detected in hypothalamic nuclei (DMD, DMV, SuMM and MM) (Fig. 2C). However, high to moderate mRNA expression was observed in cerebral cortex, distributed throughout layers I and IV in fronto-orbital cortices (113 to 180). Hybridization signals detected in both cingulate (126) and retrosplenial cortices (140) were similar to that observed in both neocortex (108) and primary olfactory cortex (106), showing a high expression in cell bodies distributed within layers II-III and IV-V, respectively). The olfactory tract (Lo) displayed the highest relative density of proMexneurin mRNA (142);

whereas moderate hybridization levels of the mRNA was observed in the nucleus accumbens (106) (Supplementary data).

### 3.4 Functional characterization of Mexneurins

**3.4.1 Mexneurins-dependent stimulation of [$^{35}$S]GTP$\gamma$S**—To assess relative agonist efficacy of peptides Mx-1, -2 and -3, we measured GPCR activation by direct activation of G$\alpha$ subunits using [$^{35}$S]GTP$\gamma$S binding. This assay assesses receptor activation by measuring guanine nucleotide exchange, an early event in GPCR-mediated signaling [20]. Mx-1 and Mx-3 as ligands stimulated the incorporation of [$^{35}$S]GTP$\gamma$S into the rat hippocampus membranes, displaying a range of potency and intrinsic activity (Fig. 3). Mx-1 stimulated [$^{35}$S]GTP$\gamma$S binding in a concentration-dependent manner, with a maximal stimulation of 86% over baseline values at 0.6 μM. Mx-3 stimulated [$^{35}$S]GTP$\gamma$S binding in a concentration-dependent manner, with a maximal stimulation of 62% over baseline values at 2.4 μM. Interestingly, high concentrations of Mx-1 (1.2, 2.4 and 4.8 μM) decreased [$^{35}$S]GTP$\gamma$S binding, an effect not observed with Mx-3 as the ligand. Mx-2 did not stimulate the incorporation of [$^{35}$S]GTP$\gamma$S (data not shown). Saturating concentrations (10 μM) of the opioid antagonist naloxone inhibited the agonist effect of Mx-1 in promoting the incorporation of $\gamma$-GTP. For Mx-3, the effect of naloxone was not evaluated because Mx-3 is not an opioid-like peptide.

**3.4.2 Electrophysiological studies**—For Mx-1, 99 cells in the rostral supraoptic nucleus (SON) and 12 cells in the suprachiasmatic nucleus (SCN) of the hypothalamus were recorded for responses to Mx-1. Due to Mx-1 sequence similarity to conserved regions of the endogenous μ-opioid agonists EM1 and EM2 [5], we examined the hypothesis that Mx-1 might display electrophysiological activity in a hypothalamic region known to respond to μ-opioid agonists. Consistent with this hypothesis, 12 cells recorded from the SCN, which has been shown to be largely unresponsive to μ-agonists [21], did not respond to Mx-1 by a reduction of spontaneous firing rate (SFR). In contrast, 32 out of 99 cells in the rostral subdivision of the SON responded to Mx-1. SFR was strongly inhibited in response to focal application of Mx-1 (Fig. 4 A), similar to previous findings using EM1 [22]. To establish a dose-response relationship of Mx-1, a total of 85 neurons were recorded in whole cell mode, of which 28 responded with an outward current (Fig. 4 B, C, D) to bath application of MX-1 at concentrations between 10 nM and 100 μM when held at a relatively depolarized membrane potential (-50 mV) compared to the average membrane resting potentials reported previously (-62 mV, [23]). Since it was difficult to determine whether neurons were responsive to Mx-1 concentrations below 10 nM (3 and 1 nM), these results were excluded from the dose-response experiments. The evoked current was dose-dependent (10 nM: 19.6 ± 3.1 pA, n = 5; 30 nM: 33.0 ± 2.1 pA, n = 3; 100 nM, 49.6 ± 6.0 pA, n = 5; 300 nM: 68.0 ± 4.2 pA, n = 3; 1 μM: 94.0 ± 13.1 pA, n = 3; 100 μM: 89.0 ± 12.6 pA, n = 3; $EC_{50}$ = 76.6 nM, Fig 4E), and reversed at –105 mV (Fig. 4 F), consistent with a K-current (calculated reversal: -103 mV). K-conductances in response to μ receptor activation have been shown in the SON [22, 24]. To examine whether Mx-1 acts through the μ receptor in the SON, we tested whether the μ receptor antagonist CTOP could inhibit the response to 100 nM Mx-1. Six SON neurons were allowed to maximally respond to bath application of Mx-1 (42.2 ± 7.2 pA). Adding CTOP (100 nM) to the bath reduced the current amplitude gradually to

$3.8 \pm 2.0$ pA. After antagonist washout, the MX-1 mediated currents returned to $31.0 \pm 8.3$ pA. Additionally, six cells in the SCN and six in the SON were tested for responses to 1 μM Mx-2 and Mx-3 each and no measurable difference in either SFR or holding current was detectable. Together, these results suggest Mx-1 may act as a μ receptor agonist.

## 4. Discussion

Our results from the immunoscreening assay show the cloning and molecular characterization of a putative mammalian protein precursor, which we named proMexneurin. The predicted polypeptide contains three potentially mature peptides, based on the rules of neuropeptide processing [19]. A single copy of an opioid-like peptide motif of 8 amino acids ($NH_2$-TFSGYPAF-$COO^-$), Mx-1, was identified in the proMexneurin protein sequence. This peptide was shown to be flanked by basic (R) and dibasic (RK) amino acids at the N-terminal and C-terminal domain, respectively of the predicted sequence, suggesting they serve as a signal site for peptide cleavage via PC1 and PC2 enzymes (See Seidah, 2011; Seidah and Prat, 2012, for reviews [25, 26]). We propose that proMexneurin is a member of type IV precursors; this group includes proteins cleaved at either single o paired residues. These proteins differ from types I-III precursors by the characteristics presence of either an R o K two residues C-terminal to cleavage site [19].

Adjacent to the dibasic cleavage signal site in the Mx-1 peptide; a second peptide of 9 amino acids ($NH_2$-TSRTDGTQS-$COO^-$) was identified, Mx-2. This peptide is flanked by a pair of basic residues (-RK- and RR-). Adjacent to Mx-2, there is an additional C-terminal peptide of 31 amino acid residues ($NH_2$-PPPRSPYSGKGLGPGNLLHSALLPIHCICLC-$COO^-$), Mx-3. This peptide showed a -CXC-like peptide motif at its C-terminus domain, similar to that found at CXC chemokines (i.e., GROα/CXCL1, PF4/CXCL4, IL-8/CXCL8, IP-10/CXCL10, SDF-1/CXCL12; see Callewaere *et al* (2007) for review [27]), suggesting that Mx-3 may represent a chemokine-like peptide.

### Distribution of Mexneurin mRNA in the Brain

To identify the tissue distribution of Mexneurin peptides in the mouse CNS and characterize a plausible Mexneurin system in the mammalian brain, we mapped the Mexneurin mRNA expression along the neuraxis of the mouse CNS. RT-PCR and *in situ* hybridization studies revealed a widespread distribution of this mRNA throughout the mouse brain. Intense expression of Mexneurin mRNA was detected in the olfactory cortex and olfactory bulb, suggesting a plausible role of Mexneurin peptides in olfactory function. Subcortical regions, such as the basal ganglia, thalamic-hypothalamic nuclei, amygdala and hippocampus showed high labeling of Mexneurin mRNA, suggesting a role of the peptides in these limbic regions. It is worth noting that the cortical regions with high proMexneurin mRNA expression—fronto-orbital, cingulate and retrosplenial—also have reciprocal innervation with thalamic areas. Furthermore, brainstem structures such as the pons and medulla exhibited high densities of proMexneurin mRNA, suggesting wide and varied regulatory roles of Mx peptides in hindbrain nuclei and cells (i.e, autonomic, cardiac and respiratory functions, alert and waking activities, sleep cycle, eating behavior, regulation of motor and sensory systems, among many others) [28, 29]. Similarly, moderate levels of Mexneurin

mRNA were detected in Purkinje cells, suggesting that Mx mRNA-derived peptides may play important physiological roles in reflex movement, balance and body equilibrium [30, 31]. Comparing the brain distribution of different opioid propeptide mRNAs to Mexneurin mRNA, the latter exhibited a grossly similar mRNA distribution with respect to that shown for prepronociceptin and proenkephalin; but fairly distinct from the prodynorphin mRNA [31]. Mexneurin mRNA was also found in hypothalamic nuclei (DMD, DMV and mamillary nucleus). Nonetheless, further studies are needed to delineate the plausible physiological roles of Mx peptides in each of these brain regions.

Opioid peptide immunoreactivity (IR) in projection fibers overlaps largely with the localization of opioid receptors (for detailed information see Le Merrer *et al* [31]). In general, major sites of Mexneurin mRNA observed in the brain matched the mRNA distribution detected for MOR [32]. However, further information is needed to assess the inmunohistochemical correlation between Mexneurinx mRNA expression and localization of Mx peptides and their cognate receptors in brain regions and neurons, respectively. In addition, the identification of the subcellular sites of expression and storage of Mexneurin peptides remains crucial to elucidate their mechanisms of action, for instance, as synaptic or non-synaptic modulators, including the plausible interaction of these peptides with other molecules involved in neurotransmission. Additionally, a single propeptide often produces multiple peptides, and propeptides may not be processed the same way in different cell types or even within the same cell type under different conditions. This is noteworthy because post-translational cleavage and post-translational modifications can affect binding affinities, as well as regulate the bioactivity and stability of the peptides [33].

## [$^{35}$S]GTP$\gamma$S binding assays

The hippocampus showed high expression of proMexneurin mRNA, and due to the structural organization of cells in compact cell layers and the stratification of afferent fibers and synapses impinging on the dendritic tree of principal cells, we used this brain area to explore [$^{35}$S]GTP$\gamma$S binding activity by Mx peptides. In this context, Mx-1 and Mx-3 stimulated the incorporation of [$^{35}$S]GTP$\gamma$S, suggesting that both peptides could act as putative ligands of GPCRs. Furthermore, stimulation of [$^{35}$S]GTP$\gamma$S by Mx-1 could imply binding activity of hippocampal mu opioid receptors [21]. Moreover, saturating concentrations of the opioid antagonist naloxone inhibited the agonist effect of Mx-1. However, stimulation of [$^{35}$S]GTP$\gamma$S incorporation by Mx-3 ligand suggests that there could be one or more GPCR binding sites for this peptide. It is interesting to note that the agonist-stimulated activity of Mx-3 was greater than that displayed by Mx-1. On the other hand, Mx-2 did not stimulate [$^{35}$S]GTP$\gamma$S incorporation (data not shown), suggesting that Mx-2 represents a non-active joining peptide.

## Electrophysiological studies

Our electrophysiological studies show that Mx-1 K-conductances evoke electrophysiological responses as a result of μ receptor activation in hypothalamic regions (i.e., SON) as previously demonstrated for EM1 and other μ-opioid agonists [22, 24]. Furthermore, the currents evoked in the SON display sensitivity to the μ-opioid antagonist CTOP. Taken

together, these results are consistent with a putative role for this peptide as an endogenous μ-opioid receptor agonist.

Accordingly to our results of the functional characterization of Mx-1 we propose that this peptide represents a hitherto unidentified opioid peptide. The opioid-like peptide motif of Mx-1 exhibits structural similarity with the consensus amino acid sequence of EMs, Tyr-Pro-Trp/Phe-Phe, with an alanine residue placed in position 3. Based on the message-address concept, opioid sequences have been subdivided into two functional parts. Thus, the message part of the N-terminal part of the peptide sequence is crucially necessary for receptor recognition, whereas the address part of the peptide motif provides the receptor selectivity [32], although, these subunits vary extremely among different opioids. Mx-1 satisfies the requirement of the general consensus of the phenolic OH group of an N-terminal Tyr residue with a free cationic α-amino group (similar to the tyramine moiety of morphine). Similarly, Mx-1 keeps an aromatic amino acid separated by one or two residues. These structural characteristics were shown to meet key requirements of opioid peptides binding to GPCRs. Furthermore, the non-acidic but the polar function of the C-terminal residue was found essential for MOR binding of endomorphins, a chemical criterion that Mx-1 peptide clearly fulfills.

Our findings suggest that further experimental work needs to be performed on Mx-1 peptide, in order to confirm its role as an opioid agonist, in addition to exploring how this peptide, may mediate its biological functions on both mu, delta and kappa opioid receptors. Furthermore, it should be interesting to explore the mechanisms of action of the Mx-1, searching for the cell-signaling pathways that this peptide may recruit when exerting its opioid and non-opioid effects in the CNS.

## Supplementary Material

Refer to Web version on PubMed Central for supplementary material.

## Acknowledgments

## Abbreviations

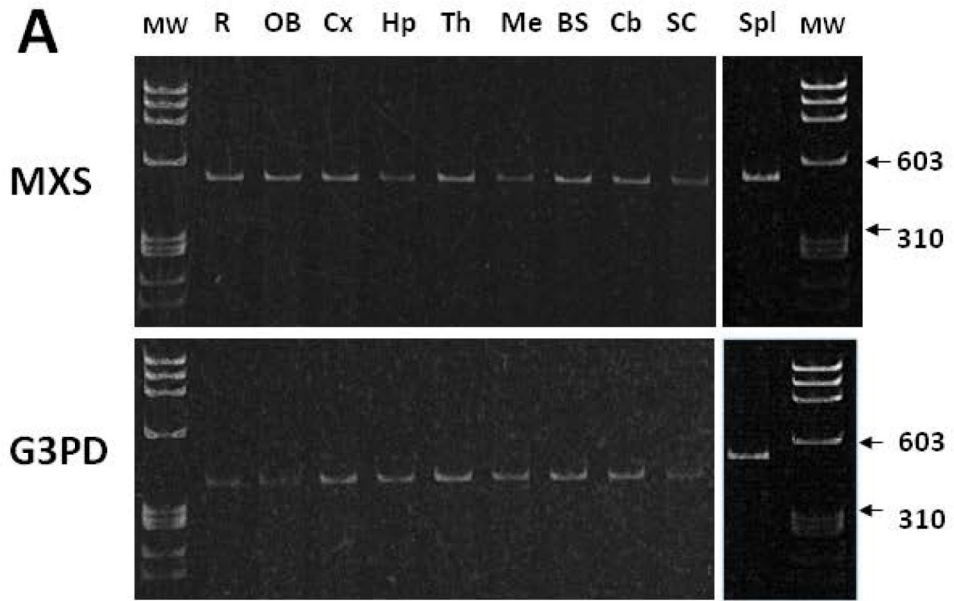| | |
|---|---|
| **EMs** | Endomorphins |
| **EM1** | Endomorphin 1 |
| **EM2** | Endomorphin 2 |
| **ORF** | Open reading frame |
| **GAPDH** | glyceraldehyde 3-phosphate dehydrogenase |

**PC1** Proconvertase 1

**PC2** Proconvertase 2

## References

1. Akil H, Watson SJ, Young E, Lewis ME, Khachaturian H, Walker JM. Endogenous opioids: biology and function. Annu Rev Neurosci. 1984; 7:223–255. [PubMed: 6324644]

2. Kieffer BL. Recent advances in molecular recognition and signal transduction of active peptides: receptors for opioid peptides. Cell Mol Neurobiol. 1995; 15:615–635. [PubMed: 8719033]

3. Meunier JC, Mollereau C, Toll L, Suaudeau C, Moisand P, Alvinerie C, Butour JL, Guillemot JC, Ferrara P, Monsarrat B, Mazarguil H, Vassart G, Parmentier M, Costentiná J. Isolation and structure of the endogenous agonist of opioid receptor-like ORL1 receptor. Nature. 1995; 377:532–535. [PubMed: 7566152]

4. Reinscheid RK, Nothacker HP, Bourson A, Ardati A, Henningsen RA, Bunzow JR, Grandy DK, Langen H Jr, Monsma FJ, Civelli O. Orphanin FQ: a neuropeptide that activates an opioidlike G protein-coupled receptor. Science. 1995; 270:792–794. [PubMed: 7481766]

5. Zadina JE, Hackler L, Ge LJ, Kastin AJ. A potent and selective endogenous agonist for the mu-opiate receptor. Nature. 1997; 386:499–502. [PubMed: 9087409]

6. Wang QP, Zadina JE, Guan JL, Shioda S. Morphological evidence of endomorphin as an agonist for the mu-opioid receptor in the rat spinal cord. Neurosci Lett. 2003; 341:107–110. [PubMed: 12686377]

7. Greenwell TN, Martin-Schild SS, Inglis FM, Zadina JE. Colocalization, shared distribution of endomorphins with substance P, calcitonin gene-related peptide, gamma-aminobutyric acid and the mu opioid receptor. J Comp Neurol. 2007; 503:319–333. [PubMed: 17492626]

8. Chen T, Hui R, Wang XL, Zhang T, Dong YX, Li YQ. Origins of endomorphin-immunoreactive fibers and terminals in different columns of the periaqueductal gray in the rat. J Comp Neurol. 2008; 509:72–87. [PubMed: 18421704]

9. Martin-Schild S, Gerall AA, Kastin AJ, Zadina JE. Differential distribution of endomorphin 1- and endomorphin 2-like immunoreactivities in the CNS of the rodent. J Comp Neurol. 1999; 405:450–471. [PubMed: 10098939]

10. Pierce TL, Wessendorf MW. Immunocytochemical mapping of endomorphin-2-immunoreactivity in rat brain. J Chem Neuroanat. 2000; 18:181–207. [PubMed: 10781736]

11. Terskiy A, Wannemacher KM, Yadav PN, Tsai M, Tian B, Howells RD. Search of the human proteome for endomorphin-1 and endomorphin-2 precursor proteins. Life Sci. 2007; 81:1593–1601. [PubMed: 17964607]

12. Anton B, Leff P, Calva JC, Acevedo R, Salazar A, Matus M, Pavón L, Martinez M, Meissler JJ, Adler MW, Gaughan JP, Eisenstein TK. Endomorphin 1 and endomorphin 2 suppress in vitro antibody formation at ultra-low concentrations: anti-peptide antibodies but not opioid antagonists block the activity. Brain Behav Immun. 2008; 22:824–832. [PubMed: 18374539]

13. Southey BR, Amare A, Zimmerman TA, Rodriguez-Zas SL, Sweedler JV. NeuroPred: a tool to predict cleavage sites in neuropeptide precursors, provide the masses of the resulting peptides. Nucleic Acids Res. 2006; 34:W267–W272. [PubMed: 16845008]

14. Logel J, Dill D, Leonard S. Synthesis of cRNA probes from PCR-generated DNA. Biotechniques. 1992; 13:604–610. [PubMed: 1476730]

15. Zheng M, Pintar JE. Analysis of ontogeny of processing enzyme gene expression and regulation. Meth Neurosc. 1995; 23:45–64.

16. Paxinos, G., Watson, C. The Rat Brain in Stereotaxic Coordinates. New York: Academic Press, Spiral Bound; 1998.

17. Selley DE, Cao CC, Liu Q, Childers SR. Effects of sodium on agonist efficacy for G-protein activation in mu-opioid receptor-transfected CHO cells and rat thalamus. Br J Pharmacol. 2000; 130:987–996. [PubMed: 10882382]

18. von Heijne G. A new method for predicting signal sequence cleave sites. Nucleic Acids Res. 1986; 14:4686–4690.

19. Seidah NG, Day R, Marcinkiewicz M, Chretien M. Precursor convertases: an evolutionary ancient, cell-specific combinatorial mechanism yielding diverse bioactive peptides and proteins. Ann N Y Acad Sci. 1998; 839:9–24. [PubMed: 9629127]

20. Sim LJ, Xiao SR, Childers R. Identification of opioid receptor-like (ORL1) peptide-stimulated [$^{35}$S]GTP gamma S binding in rat brain. Neuroreport. 1996; 7:729–733. [PubMed: 8733732]

21. Cutler DJ, Mundey R, Mason MK. Electrophysiological effects of opioid receptor activation on Syrian hamster suprachiasmatic nucleus neurones in vitro. Brain Res Bull. 1999; 50:119–125. [PubMed: 10535330]

22. Doi N, Brown CH, Cohen HD, Leng G, Russel JA. Effects of the endogenous opioid peptide, endomorphin 1 on supraoptic nucleus oxytocin and vasopressin neuroned in vivo and in vitro. Br J Pharmacol. 2001; 132:1136–1144. [PubMed: 11226145]

23. Wuarin FE, Dudek JP. Direct effects of an opioid peptide selective for μ-receptors: intracellular recordings in the paraventricular and supraoptic nuclei of the guinea-pig. Neuroscience. 1990; 36:291–298. [PubMed: 1699161]

24. Muller W, Hallermann D, Swandulla S. Opioidergic modulation of voltage-activated K+ currents in magnocellular neurons of the supraoptic nucleus in rat. J Neurophys. 1999; 81:1617–1625.

25. Seidah NG. The proprotein convertases 20 years later. Methods Mol Biol. 2011; 768:23–57. [PubMed: 21805237]

26. Seidah NG, Prat A. The biology and therapeutic targeting of the proprotein convertases. Nat Rev Drug Discov. 2012; 11:367–83. [PubMed: 22679642]

27. Callewaere C, Banisadr G, Rostène W, Parsadaniantz SM. Chemokines and chemokine receptors in the brain: implication in neuroendocrine regulation. J Mol Endocrinol. 2007; 38:355–363. [PubMed: 17339398]

28. Hendelman, W. Atlas of Functional Neuroanatomy. 3. CRC Press; 2015.

29. Orrison, WW. Atlas of Brain Function. 2. Thieme Medical Publishers; 2008.

30. Borics A, Tóth G. Structural comparison of m-opioid receptor selective peptides confirmed four parameters of bioactivity. J Mol Graph Model. 2010; 28:495–505. [PubMed: 20036591]

31. Le Merrer J, Becker JA, Befort K, Kieffer BL. Reward processing by the opioid system in the brain. Physiol Rev. 2009; 89:1379–412. [PubMed: 19789384]

32. Sharif NA, Hughes J. Discrete mapping of brain mu and delta opioid receptors using selective peptides: Quantitative autoradiography, species differences and comparison with kappa receptors. Peptides. 1989; 10:499–522. [PubMed: 2550910]

33. Mitchell JW, Atkins N Jr, Sweedler JV, Gillette MU. Direct cellular peptidomics of hypothalamic neurons. Front Neuroendocrinol. 2011; 32:377–86. [PubMed: 21334363]
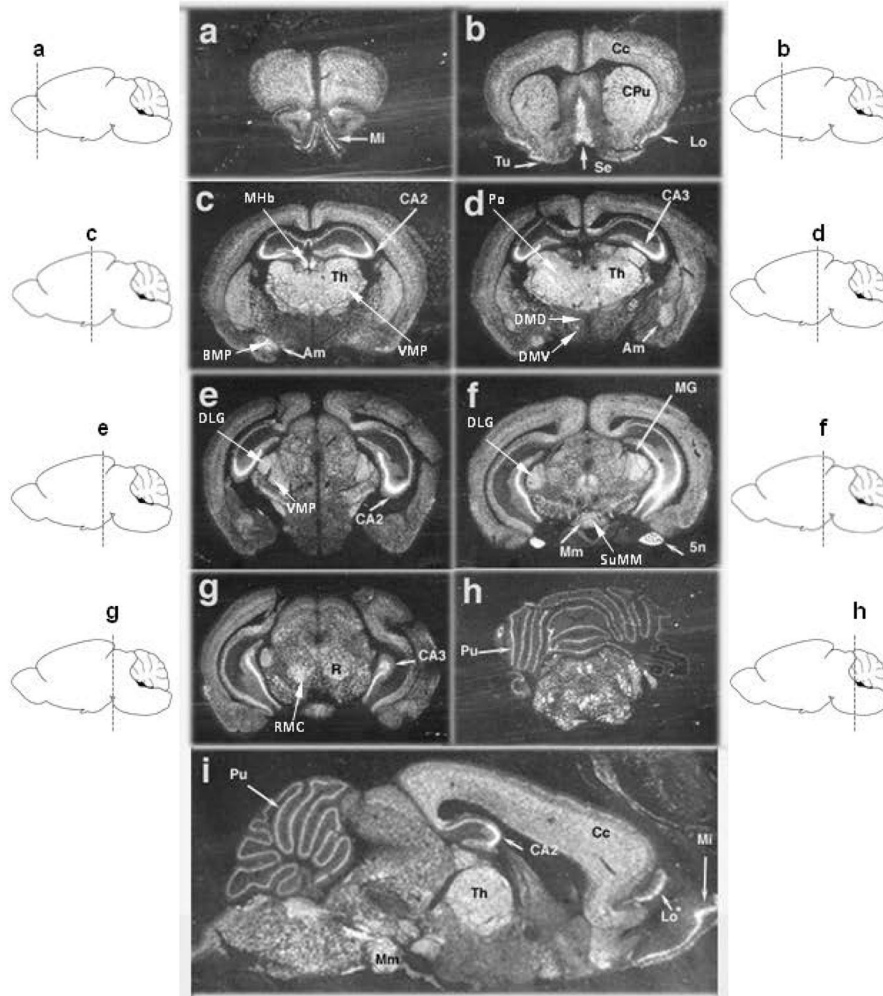
```
   1  AGAGAGGTAGCGCGCCGCGGTCCGCCGGGGTCGTCCCCCGGCGCTGCTGGCGTCCGCGCT
  61  CGGCCTGGGGAGCTGCGTGCCCTGGGGCGCAGAGGCGGCTACGGCGCGGCCAGGGCCCGG
 121  AGCCCGACTCGCCCTTCCGCCGCAGCCCGCCCCGCGGCCCCGCCTCCCCCCAGCGCTGAC
 181  CTCAGTACCCCGGACCCCTGGCCTCCCGAGGCAGGCGAGTCTCCAGGTGCGGGAGGACAG
                                         M   D   G   V   I   Y   A   E   E   S   A
 241  ACGGACGGACGGATCCAGGTGCTGGCTAGATGGACGGCGTCATCTACGCGGAGGAGTCAG
       ·  G   G   P   W   G   A   L   K   V   T   L   S   S   S   E   A   P   L   Y   G
 301  CTGGGGGTCCATGGGGGGCCCTGAAAGTGACACTAAGCTCCTCAGAGGCTCCACTCTATG
       ·  S   G   L   T   S   A   F   R   T   F   S   G   Y   P   A   F   R   K   T   S
 361  GGTCTGGACTGACTTCTGCATTCCGCACCTTCTCTGGATACCCCGCCTTCAGGAAGACTT
       ·  R   T   D   G   T   Q   S   R   R   P   P   P   R   S   P   Y   S   G   K   G
 421  CCAGGACTGACGGTACCCAGTCTCGGCGCCCTCCTCCCAGGAGCCCTTACAGTGGCAAGG
       ·  L   G   P   G   N   L   L   H   S   A   L   L   P   I   H   C   I   C   L   C
 481  GTCTGGGTCCTGGGAACTTGCTCCACTCTGCATTGCTTCCCATACACTGTATTTGCCTTT
       ·  *
 541  GCTGATACAGAGGCCCGAGATGCTCTCAGATTAGCCGAGACCGCAGCAAACATTGCCAGT
 601  GTGACCGAGAGAAGAATTTCTTCTTAAAGATAGACTCGTCATTCTGACACGTCACGGAGT
 661  CCCTGTCATCACAAGTCACAGTGTAGCTGGAGTCCCCATCGTCCCCTTCTATGTCCAGCA
 721  GATCCAGGACGCCTCTTTGAGGCAGATCATTGCTGTAGGAAAGCCCCATTTTCCTTTCCC
 781  CACTATCCTTGTCCTCCTCCTGTGAGTGAGGACATGCCTGTAGCCCCTTGCAGACAATCA
 841  GCTGCTGCCTCCTAGGGGGACACTTTTCTCAGGAAGAGGTGGCAGTAACCTCCAAAGCCA
 901  AGTTACATGCAGAAAGGCAAGCCACTTCTTGATGTATCCTGATAGAGGGAAGGAGGCACA
 961  TTTACTCCCACACCGCCCAGAACATATAGGCTTCTCTAAAGTGGCTGTATAGCGACTCAG
1021  TTCCCAACTATATACACGCAAGAAGAATAAATCGAAATAACGAGAAAAAAAAAAAAAAAA
1081  AAA
```

**Fig. 1.**

**B**

**Fig. 2.**

**Fig. 3.**

**Fig. 4.**